Journal of Applied Polymer Science

Melt processing of polyamide 12 and cellulose nanocrystals nanocomposites

Apiradee Nicharat,[1] Janak Sapkota,[1] Christoph Weder,[1] E. Johan Foster[1,2]
[1]Adolphe Merkle Institute, University of Fribourg, Fribourg, Switzerland
[2]Department of Materials Science and Engineering, Virginia Tech, Macromolecules and Interfaces Institute, Blacksburg VA
Correspondence to: E. J. Foster (E-mail: johanf@vt.edu) and C. Weder (E-mail: christoph.weder@unifr.ch)

ABSTRACT: The fabrication of nanocomposites of polyamide 12 (PA12) and cellulose nanocrystals (CNCs) isolated from cotton and tunicates is reported. Through a comparative study that involved solution-cast (SC) and melt-processed materials, it was shown that PA12/CNC nanocomposites can be prepared in a process that appears to be readily scalable to an industrial level. The results demonstrate that CNCs isolated from the biomass by phosphoric acid hydrolysis display both a sufficiently high thermal stability to permit melt processing with PA12, and a high compatibility with this polymer to allow the formation of nanocomposites in which the CNCs are well dispersed. Thus, PA12/CNC nanocomposites prepared by melt-mixing the two components in a co-rotating roller blade mixer and subsequent compression molding display mechanical properties that are comparable to those of SC reference materials. Young's modulus and maximum stress could be doubled in comparison to the neat PA12 by introduction of 10% (CNCs from tunicates) or 15% w/w (CNCs from cotton) CNCs. © 2015 Wiley Periodicals, Inc. J. Appl. Polym. Sci. **2015**, *132*, 42752.

KEYWORDS: nanoparticles; nanowires and nanocrystals; polyamides; structure–property relations; thermoplastics; thermal properties

Received 3 June 2015; accepted 21 July 2015
DOI: 10.1002/app.42752

INTRODUCTION

The use of feedstock from renewable resources appears be of growing importance for future polymer-based materials, due to environmental-impact concerns, sustainability aspects, as well as dwindling supplies of crude oil.[1] Cellulose, the most abundant renewable polymer on earth, is receiving significant attraction in this context.[2–5] While cellulose fibers have been utilized to create fabrics for thousands of years,[6,7] chemical technology enabled uses of this raw material, e.g., in the form of regenerated or chemically modified cellulose, depolymerized fragments, or hydrolytically isolated cellulose nanocrystals (CNCs),[8–10] are developments of the last century. CNCs feature dimensions of *ca.* 20 x 200–2000 nm (width x length) (depending on the source), offer high on-axis strength and stiffness, appear to be nontoxic,[11–15] and can be isolated from a plethora of biosources including wood, cotton, and many agricultural waste products.[16–22] These attractive properties, the broad range of prospective uses (*vide infra*), and need to develop new markets for the rapidly changing pulp and paper industry have triggered the recent establishment of several (pilot) plants for the production of wood-based CNCs.[23–30] CNCs have been demonstrated to be useful for the design of mechanical adaptive materials,[31–36] drug-release systems,[37,38] sensors and actuators,[39–41] biomedical devices,[42,43] self-healing materials,[44,45] aerogels,[46,47] barrier materials,[48–50] filtration membranes,[51] and many other materials systems,[52–54] but by volume, their most important potential use may be as a reinforcing filler in polymer nanocomposites.[1,55] These lightweight materials are potentially recyclable,[56] offer high strength-to-weight ratios,[28–30,57] and the approach permits one to readily tune materials properties by way of compositional variation. While several laboratory methods have been shown useful to produce polymer/CNC nanocomposites with attractive properties, few of the research-scale processes employed are technologically and industrially viable.[58–60] The main problems that prevent the successful melt-compounding of CNCs with polymers include insufficient compatibility with the polymer,[61,62] mechanical degradation of the CNCs under the high shear forces applied during thermoplastic compounding,[63,64] and thermal degradation of the CNCs during melt processing at elevated temperatures.[65,66]

Recently, Sapkota *et al.*[64] demonstrated that the mechanical degradation of CNCs can be avoided if these nanoparticles are compounded with a polymer under low-shear mixing condition, for example, in a co-rotating roller blade mixer (RBM).

Additional Supporting Information may be found in the online version of this article.

Moreover, our group has reported that thermally stable CNCs can be produced if they are isolated by hydrolysis with phosphoric and not sulfuric acid.[67] While the hydrolysis with sulfuric acid causes the introduction of a considerable amount (typically 30–90 mmol/kg) of negatively charged sulfate half-ester groups on the CNC surfaces (S-CNCs),[68] which catalyze the degradation of cellulose, especially at higher temperatures,[65,68] hydrolysis with phosphoric acid affords phosphorylated CNCs (P-CNCs) with much lower surface charge density (ca. 11 mmol/kg) and higher thermal stability.

PA12 is a semicrystalline engineering thermoplastic that displays a much lower water take-up than most other polyamides and is used in automotive applications,[69] cable,[70,71] wire and tube coatings, gas pipes,[72] barrier membranes,[72–74] and a broad range of other engineering applications.[75–79] Polyamides have been modified using a variety of fillers, including clay,[80,81] glass fibers,[82] carbon nanotubes,[83,84] graphite,[85,86] etc. Interestingly, only few studies have been reported, which address the melt-mixing of PA nanocomposites with bio-fillers. This may be related to the high temperatures required to process PAs and the comparably low decomposition temperature of many biomaterials. Kiziltas *et al.*[87] reported composites of polyamide 6 (PA6) and microcrystalline cellulose (MCC), a larger and generally round shaped form of cellulose that was created by melt-mixing the components in a twin-screw extruder. A lubricant was incorporated to facilitate mixing, and nanocomposites with high MCC loadings thus produced displayed indeed a higher storage modulus than the neat PA6. Panaitescu *et al.*[88] prepared several nanocomposites containing polyamide 11 (PA11) and cellulose nanofibers by melt-mixing at 185°C and observed slight increase in stiffness, the highest increase in Young's modulus being 41% compared to neat PA11 for nanocomposites containing 8 wt % cellulose nanofiber. However in all compositions, significant amount of agglomeration was observed. A recent study on melt-processed nanocomposites made from PA6 and CNCs isolated from cotton via sulfuric acid hydrolysis showed that melt processing was possible when the CNCs were first coated with polymer solution and then dried to protect them from thermal degradation during melt mixing.[89] An extruded and injection-molded nanocomposite with a CNC concentration of 1 wt % did indeed increase the elastic modulus of nanocomposite by 45% (to ~1900 MPa) compared to neat PA6 (~1290 MPa), attributed to better dispersion and better interfacial adhesion promoted by coating the CNCs with polymer. However, no detailed characterization and no high content CNC nanocomposites were reported, hence it is unclear whether similar behavior can be obtained with greater amounts of CNCs in the system.

Building on these advances, and speculating that the combination of polar and nonpolar motifs found in polyamide 12 (PA12) would promote good compatibility with CNCs, we set out to study melt-mixed (MM) nanocomposites of PA12 and CNCs isolated from cotton and tunicates. Through a comparative study that involved SC and melt-processed materials, it was shown how PA12/CNC nanocomposites with high mechanical properties can be prepared in a process that appears to be readily scalable to an industrial level. Our experiments demonstrate that CNCs isolated from the biomass by phosphoric acid hydrolysis display both a sufficiently high thermal stability to permit additive-free melt processing with PA12, and a high compatibility with this polymer to allow the formation of nanocomposites in which the CNCs are well dispersed. This approach appears to represent the most proficient and scalable method for the production of PA/CNC nanocomposites, and it may also be applicable to other thermoplastic polymers.

EXPERIMENTAL

Materials

PA12 (Ubesta 3024 U, received from UBE) having a weight-average molecular weight, Mw, of 24 000 g/mol and density $\delta = 1.04$ g cm^{-3} was obtained in the form of solid pellets from UBE America Inc. Cotton-derived cellulose nanocrystals (cCNCs) were isolated from Whatman No. 1 filter paper via sulfuric acid (S-cCNCs) and phosphoric acid hydrolysis (P-cCNCs) using the previously reported procedures.[67,90,91] Tunicates, *Styela clava*, were collected from floating docks at Port de Plaisance du Moulin Blanc, France. The tunicates were cleaned and bleached as previously reported.[31] Sulfated tunicate cellulose nanocrystals (S-tCNCs) were isolated using sulfuric acid hydrolysis as the previously reported procedure.[31,44,66]

Isolation of Cellulose Nanocrystals by Phosphoric Acid Hydrolysis of Tunicate Mantles

Phosphorylated tunicate cellulose nanocrystals (P-tCNCs) were prepared from bleached tunicate mantles in a protocol that adapts the procedure developed by Camarero Espinosa *et al.* for cotton-based CNCs.[67] The bleached and dried mantles (2 g) were soaked in purified water (200 mL) from a milliQ Sartorius arium 611VF overnight and disintegrated in a kitchen blender at high speed for 15 min, yielding a fine cellulose pulp. Phosphoric acid (95–97%, 350 mL) was slowly added under vigorous mechanical stirring to the cellulose pulp, which was cooled in an ice bath; the addition was controlled so that the temperature was kept below 20°C. After 300 mL of the acid had been added, the dispersion was removed from the ice bath and was heated to 40°C during the addition of the final 50 mL of acid. After the acid addition was complete, the mixture was heated to 100°C and was kept at this temperature for 90, 150, 180, or 210 min under continuous stirring in order to establish the optimum hydrolysis time. After the hydrolysis was complete, the mixture was cooled to room temperature, centrifuged (20 min at 3600 rpm), and the supernatant was decanted. Deionized water was added and the centrifugation step was repeated at least three times until the pH of the dispersion reached ~5. After the last centrifugation, the resulting P-tCNCs were dialyzed against H_2O for 7 days; during this process, the H_2O was exchanged twice per day. The CNC suspension was subsequently diluted with deionized water (total volume 500 mL) and sonicated in a Badelin Sonorex Technik RL 70 UH ultrasound bath for 18 h at 25°C, before it was filtered through a No. 1 glass filter in order to remove any remaining aggregates. The concentration of the CNCs in the final dispersion was determined gravimetrically to be ~3 mg/mL. This dispersion was freeze-dried using a VirTis BenchTop 2K XL lyophilizer with an initial temperature of 25°C and a condenser temperature of −78°C.

Table I. Characteristics of the CNCs Used

Property	S-cCNCs	S-tCNCs	P-cCNCs	P-tCNCs
Charge concentration[a] (mmol/kg)	95	80	10	30
Length[b] (nm)	295±115	1850±530	320±110	2300±760
Diameter[b] (nm)	24±5	28 ± 10	30 ± 5	35 ± 12
Aspect ratio[b] (-)	13±2.15	76 ± 20	13±2.5	80±15

[a] Determined by conductometric titration.
[b] Determined by evaluation of transmission electron microscopy images.

H_2O was removed during 72 h. P-tCNCs thus produced were kept in an air-tight container and were used as needed. Based on image analysis of the obtained P-tCNCs (Supporting Figures S1, S2), a hydrolysis time of 210 min was selected as an optimal method because of high CNC yield after hydrolysis and better variation in aspect ratio compared to other hydrolysis time. P-tCNCs used in this study were prepared accordingly.

Conductometric Titration of CNCs

In order to determine their surface charge density, all CNCs used in this study were titrated using the conductometric titration technique reported by Camarero Espinosa *et al.*[67] Thus, 50 mg of the CNCs were suspended in 10–15 mL of 0.01*M* aqueous hydrochloric acid. After 5 min of stirring and 20 min of sonication (in a Badelin Sonorex Technik RL 70 UH), the suspensions were titrated with 0.01*M* NaOH. The phosphate-ester and sulfate-ester contents were determined from the volume of NaOH required to titrate the sample, and normalizing it to the weight of the sample using a similar approach to the one described for S-cCNCs.[67,92] The surface charge densities determined were as follows: S-cCNCs: 95 mmol/kg, S-tCNCs: 80 mmol/kg. P-cCNCs: 10 mmol/kg. P-tCNCs: 30 mmol/kg.

Preparation of PA12/CNC Nanocomposites by Melt Mixing

PA12/CNC nanocomposites with a CNC content of 5%, 10%, 15%, and 20% w/w were prepared by direct melt mixing in a RBM (Brabender® GmbH & Co. KG, Duisburg, Germany; mixer type 30EHT). The temperature and rotor speed were set to 190°C at 70 rpm, respectively. The polymer was first introduced to the RBM and processed until it had transformed into a viscous melt (~6 min). The CNCs were added at this point and mixing was continued for a further 4 min. The nanocomposites were removed from the mixer and allowed to cool to the room temperature. The materials were subsequently compression-molded between poly(tetrafluoroethylene) sheets in a Carver® press at 190°C under a pressure of 3 metric tons for 5 min. The thickness of the films was controlled by the use of spacers to a typical value of 200 μm, as measured with a caliper. A neat PA12 film was also prepared by melt-mixing under analogous conditions.

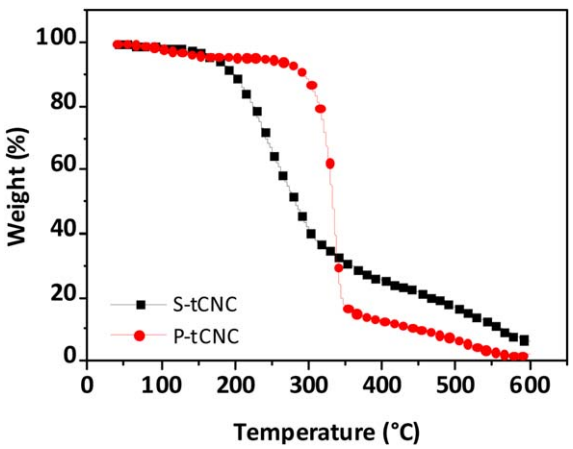

Figure 1. TGA thermograms of S-tCNCs and P-tCNCs under nitrogen. The measurements were conducted at a heating rate of 10°C min^{-1}). [Color figure can be viewed in the online issue, which is available at wileyonlinelibrary.com.]

Preparation of PA12/CNC Nanocomposites by Solution Casting

Freeze-dried CNCs were dispersed in N,N-dimethylformamide (DMF, extra dry over molecular sieves, purchased from Acros Organics, at a concentration of 5 mg mL^{-1} by sonication for 4 h in an ultrasonic bath (Badelin Sonorex Technik RL 70 UH). PA12 was dissolved in DMF at a concentration of 15% w/w by stirring the mixture at 120°C for 4 days. The appropriate amount of CNC dispersion was added to the PA12 solution. For example, for a 15% w/w nanocomposite, 25 mL of a 15% w/w PA12 solution was added to 83.3 mL of a CNC dispersion in DMF. The mixtures were stirred with a magnetic stir bar under reflux conditions for 1 days before they were cast into 12.7 cm diameter Teflon® Petri dishes. The samples were placed into an oven at 70°C for 4 days to evaporate most of the solvent. The resulting films were dried in a vacuum oven at 70°C and a pressure of 400 mbar for 2 days to remove any remaining solvent. Neat PA12 films and nanocomposites containing 0% and 15% w/w CNCs were thus produced. The materials were subsequently compression-molded between poly(tetrafluoroethylene) sheets in a Carver® press at 190°C under a pressure of 3 metric tons for 5 min. The thickness of the films was controlled by the use of spacers to a typical value of 200 μm, as measured with a caliper.

Atomic Force Microscopy (AFM)

Atomic force microscopy was carried out on a NanoWizard II (JPK Instruments) microscope. The samples (neat PA12 and nanocomposites) were prepared by compression molding films of a thickness of less than 50 μm and were mounted on glass slides for film stability. The scans were performed in AC mode in air, using silicon cantilevers (NANO WORLD, TESPA-50)

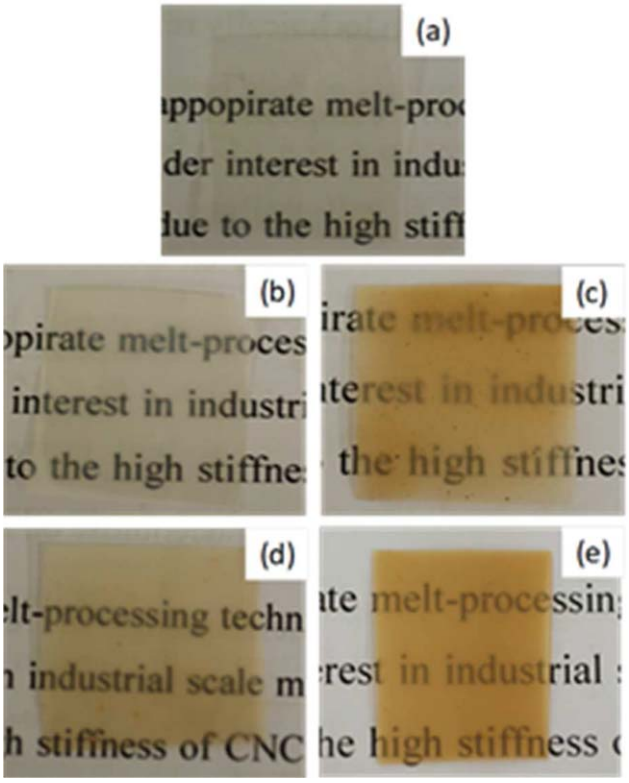

Figure 2. Pictures of compression-molded thin films of the neat PA12 (a), and PA12/CNC nanocomposites containing 10% w/w P-cCNCs (b), S-cCNCs (c), P-tCNCs (d), or S-tCNCs (e). [Color figure can be viewed in the online issue, which is available at wileyonlinelibrary.com.]

and applying a resonance frequency of 320 kHz and a scan rate of 1 line/s.

Transmission Electron Microscopy (TEM)

Lyophilized CNCs were dispersed in deionized water at a concentration of 0.08 mg/mL by sonication in a Badelin Sonorex Technik RL 70 UH ultrasonication bath for 10 min. Subsequently, the aqueous CNC dispersions were deposited on carbon-coated grids (Electron Microscopy Sciences, one drop each), and the samples were dried at 70°C for 3 h. The samples were examined by transmission electron microscopy (TEM) using a Hitachi H-1700 microscope operating at an accelerating voltage of 75 kV. The dimensions of the CNCs were determined from the TEM images by using image analysis software ImageJ. The length and width of 100 CNCs from each of 5–10 TEM images were determined; the averaged values are reported.

Dynamic Mechanical Analysis (DMA)

The mechanical properties of the PA12/CNC nanocomposites were characterized by dynamic mechanical analysis (DMA) using a TA Instruments Model Q800. The samples were prepared by cutting rectangular strips with a width of ~6 mm from the films. Tests were conducted in tensile mode using a temperature sweep method (−120 to −220°C) at a fixed frequency of 1 Hz, a strain amplitude of 15 μm, a heating rate of 10°C min^{-1}, and a gap distance between the jaws of ~10 mm.

Tensile Measurements

Tensile measurements of PA12/CNCs nanocomposites were performed using a Zwick/Roell Z010 tensile tester. Tests were carried out at room temperature with a strain rate of 5% min^{-1}, a preload force of 0.01*N*, a gap distance between the jaws of 35 mm, and using dog-bone shaped films having a width of 4 mm. Tensile moduli were calculated from the slopes of the linear region between 0.5% and 1% strain. Tensile toughness was determined by integrating the stress–strain curve.

Differential Scanning Calorimetry (DSC)

Differential scanning calorimetry measurement were performed under N_2 using a Mettler-Toledo STAR system. The typical procedure included heating and cooling cycles of approximately 8 mg sample in a DSC pan from −50°C to 250°C using a heating rate of 10°C/min. The glass transition temperature (T_g) was determined from the midpoint of the specific heat increment at the glass−rubber transition, while the melting temperature (T_m) was taken as the highest temperature point of the melting endotherm.

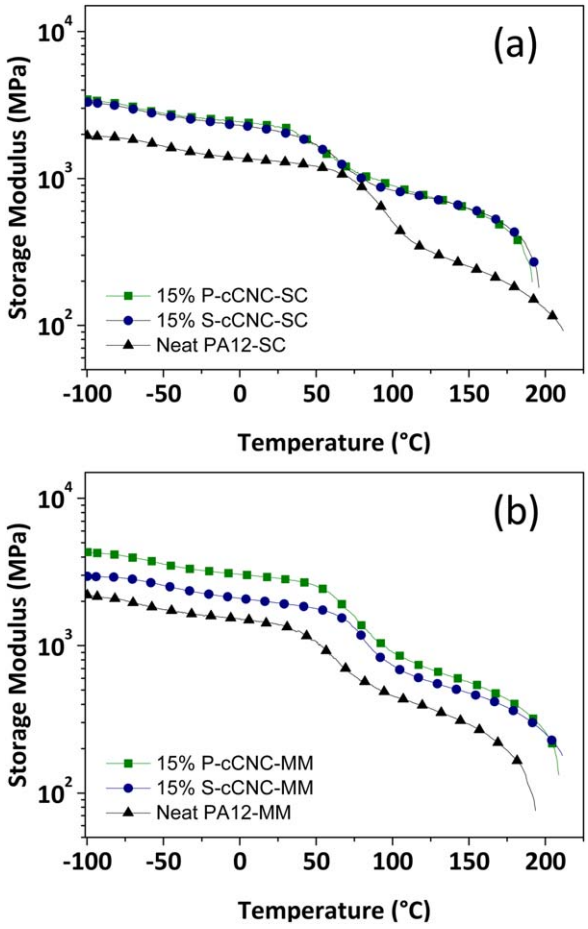

Figure 3. Dynamic mechanical analysis traces showing the storage modulus (E') of PA12 and PA12/CNC nanocomposites containing 15% w/w of P-cCNC and S-cCNC as a function of temperature. The nanocomposite films were prepared by (a) solution cast and (b) melt-mixing technique. [Color figure can be viewed in the online issue, which is available at wileyonlinelibrary.com.]

Table II. Mechanical Properties of Neat PA12 and PA12/CNC Nanocomposites at 25°C

CNC content (% w/w)	Young's Modulus (MPa)[a]	Maximum stress (MPa)[a]	Tensile toughness (10^{-4} J m^{-3})[a]	Storage modulus (MPa)[b]
0% (neat PA12)	1200 ± 100	40 ± 4	7280 ± 100	940 ± 115
5% S-cCNC	1520 ± 150	48 ± 3	1330 ± 95	1180 ± 165
5% P-cCNC	1770 ± 60	52 ± 5	300 ± 80	1430 ± 140
10% S-cCNC	1640 ± 120	55 ± 4	625 ± 70	1330 ± 185
10% P-cCNC	1790 ± 105	60 ± 4.0	310 ± 90	1450 ± 135
15% S-cCNC	2385 ± 270	63 ± 3	970 ± 115	2100 ± 270
15% P-cCNC	2400 ± 235	72 ± 3	255 ± 110	2550 ± 185
20% S-cCNC	-	-	-	1265 ± 270
20% P-cCNC	-	-	-	1650 ± 225
5% S-tCNC	1875 ± 120	50± 3	750 ± 120	1780 ± 295
5% P-tCNC	2040 ± 200	54 ± 3	530 ± 100	1950 ± 275
10% S-tCNC	2310 ± 75	65 ± 3	1030 ± 140	2230 ± 340
10% P-tCNC	2750 ± 130	80 ± 10	650 ± 130	3092 ± 165

[a] Determined by tensile testing.
[b] Determined by DMA measurements.
These samples showed phase separation and were excluded from tensile testing. All data represent averages (number of individual measurement, $N = 3$–4) ± standard error measurements.

Thermogravimetric Analyses (TGA)

The thermal stability of CNCs was probed by thermogravimetric analysis using a Mettler-Toledo STAR thermogravimetric analyzer in the range of 25–500°C with a heating rate of 10°C min^{-1} under nitrogen. The mass of the samples was ~5 mg.

Determination of Chemical Composition

The chemical composition of the P-tCNCs produced was determined by Fourier transform infrared spectroscopy (FTIR) spectroscopy. Spectra were recorded on a Perkin Elmer Spectrum 65 FTIR spectrometer r between 4000 and 600 cm^{-1} at a resolution of 4 cm^{-1} and a total of 15 scans.

RESULTS AND DISCUSSION

The CNCs used in this study were isolated from cotton and tunicates (*Styela clava*) collected from the French Atlantic coast. While the former have dimensions and mechanical properties that are comparable to CNCs isolated from soft pulp wood and represent an excellent model for a commercially viable CNC type, the latter are of interest because of their superior mechanical properties and higher aspect ratio, which bestow tCNCs with superior reinforcing capability.[31,44,58,93] In order to enable a direct comparison, we employed CNCs isolated by sulfuric acid hydrolysis using standard protocols (S-cCNCs[94,95] and S-tCNCs),[34,96,97] as well as CNCs isolated by hydrolysis with phosphoric acid (P-cCNCs[67,98,99] and P-tCNCs). While P-cCNCs were prepared using the method previously reported by Camarero Espinosa *et al.*,[67] P-tCNCs were so far unknown. By increasing the hydrolysis time, we were able to adapt the hydrolysis conditions reported for the isolation of P-cCNCs[67] to the isolation of P-tCNCs from tunicate mantles. Table I, which summarizes the dimensions and surface charge density of all CNC types used in this study, shows that P-tCNCs feature similar dimensions as S-tCNCs, but a surface charge density that is much lower, and similar to that found in P-cCNCs.

The thermal stability of the new P-tCNCs was determined by thermogravimetric analysis (TGA); S-tCNCs were measured for reference purposes. As shown in Figure 1, the degradation of S-tCNCs (defined as temperature at which the weight loss is 5%) sets in around 180°C, which is consistent with previous reports.[68] The degradation temperature of P-tCNCs was established to be 290°C (Figure 1). The significantly improved thermal stability of P-tCNCs *vis à vis* S-tCNCs mirrors the behavior observed for the corresponding c-CNCs[67] (Supporting Figure S4) and is, as will be shown below, decisive for successful melt processing with PA12 at 190°C. Recent studies have shown that neutralizing acid sulfate group content of CNCs after hydrolysis using strong base could recover the thermal stability of CNCs once the neutral pH is reached; however, the TGA analysis shows the thermal stability of S-cCNCs neutralized using NaOH is better than S-cCNCs but still unable to compete with P-cCNC.[46,100]

Previous research in our group has previously shown the versatility of solution-casting mixtures of polymers such as poly(vinyl acetate),[34,35,64] poly(vinyl alcohol),[31] poly(ethylene oxide-*co*-epichlorohydrin),[96] or poly(urethane)[101] and CNCs from dimethylformamide and optionally subsequent compression molding affords nanocomposite films with homogenously dispersed CNCs.[34,35,45,64,102] In the dry state, these materials display mechanical properties that are attributed to the formation of three-dimensional hydrogen-bonded CNC networks within the polymer and their stiffness is well described by a percolation model.[103,104] Thus, we opted to utilize solution casting of PA12/CNC mixtures and subsequent compression-molding to produce reference nanocomposites with the presently investigated CNC types. These experiments were conducted with a CNC

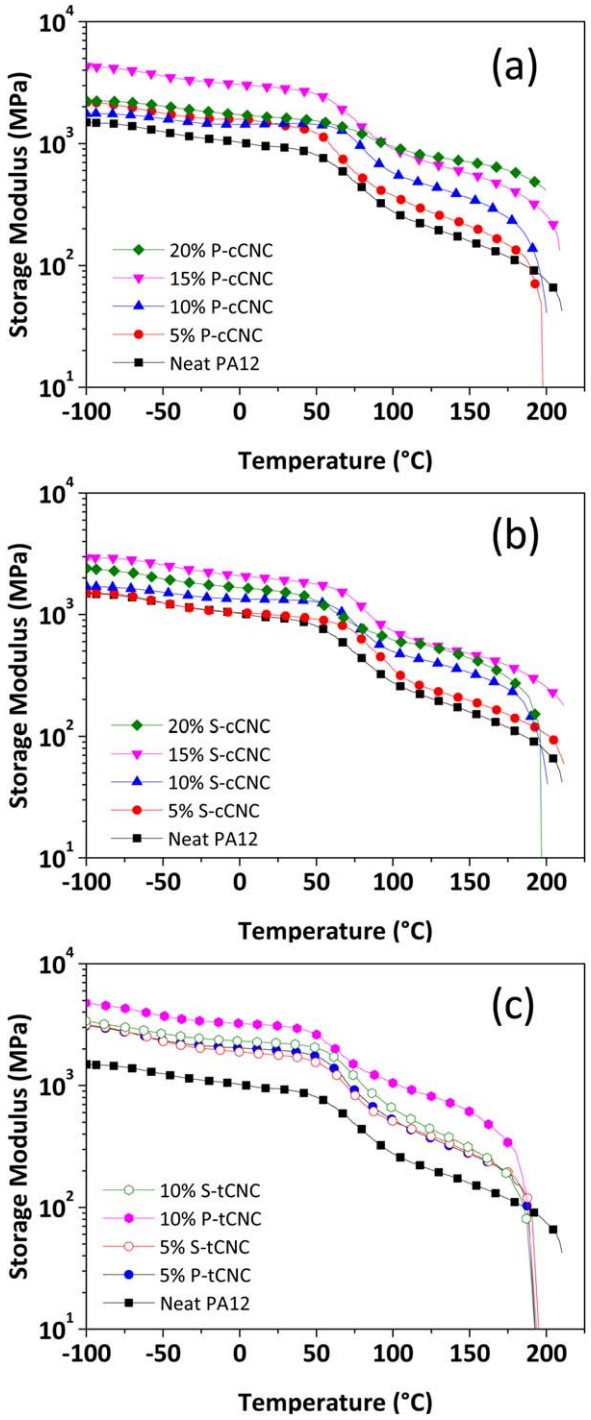

Figure 4. Dynamic mechanical analysis traces showing the storage modulus (E') of PA12 and PA12/CNC nanocomposites containing various amounts of S-cCNCs (a), P-cCNCs (b), P-CNCs or S-tCNCs (c) as function of temperature. All samples were prepared by melt mixing and subsequent compression molding. [Color figure can be viewed in the online issue, which is available at wileyonlinelibrary.com.]

content of 15% w/w and the SC samples were re-processed by compression molding into ~200 μm thin films. PA12/CNC nanocomposites with varying CNC content (5%, 10%, 15%, and 20% w/w) were also prepared by directed melt-mixing in a RBM. The PA12 was first melted in the RBM at 190°C, before CNCs were added and the mixture was compounded for 4 min. The nanocomposites were removed, allowed to cool to room temperature, and the materials were compression molded at 190°C to produce ~200 μm thin films.

Photographs of the melt-processed nanocomposite films (Figure 2) containing 10% w/w of the four CNC types (P-cCNCs, S-cCNCs, P-tCNCs, and S-tCNCs) provide a first indication of the higher thermal stability of the phosphorylated over the sulfated CNCs. It is clearly apparent that the nanocomposites containing S-cCNCs or S-tCNCs darken considerably, in contrast to the composites with either of the phosphated CNC types, which remain virtually colorless. While the qualitative nature of the experiments does not permit further conclusions, the observed color gradient (neat PA12 $\approx$ PA12/P-cCNC < PA12/P-tCNC < PA12/S-cCNC < PA12/S-tCNC) follows the concentration of surface ester groups and confirms the previously derived conclusion that not only their nature, but also concentration determines the CNCs thermal stability.[67] The nanocomposite containing neutralized S-cCNCs also showed the yellowing effect, the color qualitatively being midway between that of S-cCNCs and P-cCNCs, due to the corresponding intermediate thermal stability as confirmed by TGA.

Let us first focus on nanocomposites based on cCNCs. We first compared the mechanical properties of compression-molded films made from MM and SC PA12/CNC nanocomposites containing 15% w/w of P-cCNCs or S-cCNCs. The data were acquired by DMA (Figure 3) and the neat PA12 was also measured. Figure 3(a) shows that both SC nanocomposites show identical DMA traces and that both materials exhibit an increased storage modulus (E') in comparison to the neat PA12 both above and below the glass transition temperature (T_g). This behavior matches the previous results for cellulose-reinforced polymers of this type,[89,105] and suggest that solution casting affords well-dispersed nanocomposites. We note that DSC curves of MM neat PA12 and solution cast PA12, that were compression molded afterwards, showed similar behavior as shown in Figure S5, suggesting the processing method had no significant influence on structure. A similar trend was observed for the MM nanocomposites containing either S-cCNCs or P-cCNCs (Figure S6). As suspected on the basis of the lower thermal stability of S-cCNCs and subsequently MM nanocomposites containing S-cCNCs (Supporting Figure S7) display, at all temperatures, a lower stiffness than the corresponding materials with P-cCNCs [Figure 3(b)]. For example, at 25°C, E' of the melt-processed 15% w/w PA12/P-cCNC nanocomposite is 2600 MPa, whereas the value for the corresponding S-cCNC sample is only 2100 MPa (Table II). The fact that the DMA data of the MM and SC P-cCNC nanocomposites are virtually identical over the entire temperature regime suggests that both processes result in a similar nanocomposite structure, in which the CNCs are well dispersed in the PA12 matrix. Similar reinforcement as of S-cCNCs was obtained when neutralized S-cCNCs were used to obtain nanocomposites and hence for further analysis only S-cCNCs and P-cCNCs were used.

We next investigated the influence of the CNC concentration on the reinforcement of MM nanocomposites containing P-cCNCs

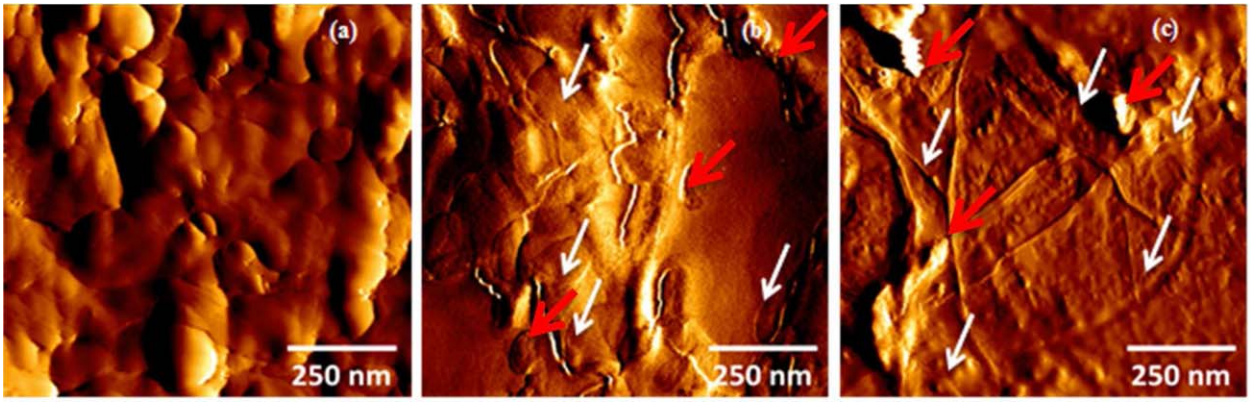

Figure 5. AFM amplitude images of 50 μm thin films of neat PA12 (a), and melt-mixed nanocomposites of PA12 and 15% w/w P-cCNCs (b) or 15% w/w S-cCNCs (c). Scale bar = 250 nm. The white arrows show individual CNCs dispersed in the polymer matrix, red arrows shows aggregates of CNCs. [Color figure can be viewed in the online issue, which is available at wileyonlinelibrary.com.]

or S-cCNCs (Table II). In the case of the P-cCNC-based nanocomposites, E' rose with the CNC content. At 25°C, E' increased from ~950 MPa for the neat PA12 to ~2500 MPa for the composite with 15% w/w CNCs [Figure 4(a)]. The S-cCNC series shows a similar behavior, but the reinforcing effect is less pronounced; here, the 15% w/w PA12/S-cCNC nanocomposite shows an E' of only ~2100 MPa [Figure 4(b)]. The reduced reinforcement of the S-cCNC series mirrors the situation discussed above for the 10% w/w PA12/S-cCNC composite and is consistent with (partial) degradation of the S-cCNC surface and/or aggregation effects. In both cases, the nanocomposites containing 20% w/w CNCs displayed a lower E' than the materials with 15% w/w CNCs (P-cCNC: 1650 MPa; S-cCNC: 1250 MPa), likely due to the aggregation and phase separations when a higher content of CNCs is incorporated. An incremental increase in the Young's modulus is observed with addition of CNCs from 1200 MPa for neat PA12 to 2400 MPa for nanocomposite comprising 15% w/w P-cCNCs. The Young's modulus shows the similar pattern as storage modulus (see Table II), with increases observed when greater amounts of CNCs are mixed into the system. As expected, elongation at break for the nanocomposites decreases with addition of CNCs from ~220% in the case of neat PA12 to ~20% for the nanocomposites containing 15% w/w P-cCNCs. Correspondingly, with an increase in stiffness and decrease in elongation at break, the toughness was reduced from 7300 10^{-4} J m^{-3} for neat polymer to 250 10^{-4} J m^{-3} for nanocomposites containing 15% w/w P-cCNCs.

To confirm the level of homogeneity and CNC dispersion in the MM PA12/cCNC nanocomposites, atomic force microscopy (AFM) experiments were carried out on samples containing either 15% w/w P-cCNCs or S-cCNCs (Figure 5). In comparison to the surface of neat PA12 film [Figure 5(a)], the AFM image of the nanocomposite containing P-cCNCs [Figure 5(b)] clearly shows well-dispersed, individualized CNCs even at 15% w/w filler content (indicated by white arrows). By contrast, the presence of some CNC aggregates (in nanocomposites containing S-cCNCs [Figure 5(c)] can be observed.

Taken together, the data seem to suggest a much better dispersibility and thermal stability of the P-cCNCs in the PA12 matrix than in the case of the S-cCNCs, at least up to a CNC content of 15% w/w. When the CNC content was increased to 20% w/w, all samples had a heterogeneous appearance (Figure S12), which is explained by CNC aggregation.

Finally, we explored the possibility to reinforce PA12 with 5% or 10% w/w CNCs extracted from tunicates (tCNCs). Figure 4(c) and Table II show that these two series show the same trends as the cCNC series (larger reinforcing effect of P-tCNCs than S-tCNCs). As expected from the large body of work that enables a comparison of tCNC and cCNC based nanocomposites, the former displays a much higher reinforcing power.[106,107] For example at 25°C, the 10% w/w PA12/S-tCNC nanocomposite displays an E' of ~2200 MPa, whereas the nanocomposites containing 10% w/w S-cCNCs features an E' of ~1300 MPa. Similarly at 25°C, the 10% w/w PA12/P-tCNC-nanocomposite MM displays an E' of ~3100 MPa, whereas the nanocomposites containing 10% w/w P-cCNCs-MM features an E' of ~1500 MPa. Overall, the t-CNCs demonstrates a higher reinforcing capability than their lower-aspect ratio counterpart isolated from cotton, possibly due to not only the higher aspect ratio, but also a higher on-axis stiffness of individual CNCs.[33,97,108]

The thermal properties of compounded nanocomposites, glass transition temperature (T_g), melting temperature (T_m) (of PA components), crystallization temperature (T_c), and degradation temperature (T_d) were analyzed by DSC and TGA (see Figure S4). Interestingly, for all of the PA12 and composite systems, the exothermic peak becomes wider with a relatively small change in the crystallization and melting peak temperatures, so the addition of CNCs did not significantly affect the degree of crystallization of PA12.

CONCLUSIONS

In summary, we show that thermally stable CNCs isolated via phosphoric acid hydrolysis can be melt mixed into PA12 without the need for additives or costly surface grafting. The substantial doubling of maximum stress and Young's modulus relative to the neat polymer indicate that the introduction of 10% (CNCs from tunicates) or 15% w/w (CNCs from cotton)

CNCs at a mixing temperature of 190°C facilitated P-CNCs to be efficiently mixed into the semi-crystalline PA12. The excellent mechanical and thermal properties of lightweight bio-based fillers nanocomposites are useful in numerous applications, such as automotive parts, ski boots, and electrical appliance: applications that require lower weight or replacing glass fiber- reinforced material. This approach represents a significant step in improving a new industrially scalable processing method for CNC nanocomposites, and the production of bio-based fillers combined with PA12.

ACKNOWLEDGMENTS

The authors gratefully acknowledge the financial support from the Swiss National Science Foundation (NRP66: Resource Wood, Nr. 406640_136911/1) and the Adolphe Merkle Foundation. Author E.J.F. is visiting Professor in LabEx Tec 21, Grenoble, France (Investissements d'Avenir—grant agreement n°ANR-11-LABX-0030).

REFERENCES

1. Peng, B. L.; Dhar, N.; Liu, H. L.; Tam, K. C. *Can. J. Chem. Eng.* **2011**, *89*, 1191.
2. Habibi, Y.; Lucia, L. A.; Rojas, O. *J. Chem. Rev.* **2010**, *110*, 3479.
3. Beck-Candanedo, S.; Roman, M.; Gray, D. G. *Biomacromolecules* **2005**, *6*, 1048.
4. Moon, R. J.; Martini, A.; Nairn, J.; Simonsen, J.; Youngblood, J. *Chem. Soc. Rev.* **2011**, *40*, 3941.
5. Lin, N.; Dufresne, A. *Eur. Polym. J.* **2014**, *59*, 302.
6. Maren, R. "Model Cellulosic Surfaces: History and Recent Advances", in Model Cellulosic Surfaces, American Chemical Society, **2009**, p. 3.
7. Klemm, D.; Kramer, F.; Moritz, S.; Lindström, T.; Ankerfors, M.; Gray, D.; Dorris, A. *Angewandte Chem. Int. Ed.* **2011**, *50*, 5438.
8. Jiang, F.; Esker, A. R.; Roman, M. *Langmuir* **2010**, *26*, 17919.
9. Luiz de Paula, E.; Mano, V.; Pereira, F. V. *Polym. Degrad. Stab.* **2011**, *96*, 1631.
10. Serizawa, T.; Sawada, T.; Okura, H.; Wada, M. *Biomacromolecules* **2013**, *14*, 613.
11. Endes, C.; Muller, S.; Schmid, O.; Vanhecke, D.; Foster, E.; Petri-Fink, A.; Rothen-Rutishauser, B.; Weder, C.; Clift, M. *J. Phys. Conf. Ser.* **2013**, *429*, 012008.
12. Endes, C.; Schmid, O.; Kinnear, C.; Mueller, S.; Camarero-Espinosa, S.; Vanhecke, D.; Foster, E.; Petri-Fink, A.; Rothen-Rutishauser, B.; Weder, C.; Clift, M. *Particle Fibre Toxicol.* **2014**, *11*, 40.
13. Yanamala, N.; Farcas, M. T.; Hatfield, M. K.; Kisin, E. R.; Kagan, V. E.; Geraci, C. L.; Shvedova, A. A. *ACS Sustain. Chem. Eng.* **2014**, *2*, 1691.
14. Hanif, Z.; Ahmed, F. R.; Shin, S. W.; Kim, Y.-K.; Um, S. H. *Colloids Surf. B: Biointerf.* **2014**, *119*, 162.
15. Milton, D. K.; Godleski, J. J.; Feldman, H. A.; Greaves, I. A. *Am. Rev. Respir. Dis.* **1990**, *142*, 184.
16. De Souza Lima, M.; Borsali, R. *Macromol. Rapid Commun.* **2004**, *25*, 771.
17. Klemm, D.; Kramer, F.; Moritz, S.; Lindstrom, T.; Ankerfors, M.; Gray, D.; Dorris, A. *Angewandte Chem. Int. Ed.* **2011**, *50*, 5438.
18. Orts, W. J.; Shey, J.; Imam, S. H.; Glenn, G. M.; Guttman, M. E.; Revol, J. F. *J. Polym. Environ.* **2005**, *13*, 301.
19. Domingues, R. M. A.; Gomes, M. E.; Reis, R. L. *Biomacromolecules* **2014**, *15*, 2327.
20. Mariano, M.; El Kissi, N.; Dufresne, A. *J. Polym. Sci. Part B: Polym. Phys.* **2014**, *52*, 791.
21. Aspler, J.; Bouchard, J.; Hamad, W.; Berry, R.; Beck, S.; Drolet, F.; Zou, X. Review of Nanocellulosic Products and Their Applications, in Biopolymer Nanocomposites, First ed., Eds. Dufresne, A., Thomas, S., and Pothen, L.A., **2013**, p 461, John Wiley & Sons, Inc: New Jersey.
22. Dufresne, A. *Int. Polym. Process.* **2012**, *27*, 557.
23. Peresin, M. S.; Habibi, Y.; Zoppe, J. O.; Pawlak, J. J.; Rojas, O. *J. Biomacromolecules* **2010**, *11*, 674.
24. Oksman, K.; Mathew, A. P.; Bondeson, D.; Kvien, I. *Compos. Sci. Technol.* **2006**, *66*, 2776.
25. Rudie, A. W.; Yu, Y.; Rudie, A.; Cai, Z.; Anderson, R.; Reid, D.; Hart, P.; Hart, P. W. In Proceedings of the International Conference on Woody Biomass Utilization, Starkville, MS, 4–5 August, 2009. Ed. John R. Shelly, Forest Products Society, Madison, WI, ISBN-13: 978-1-892529-60-2; **2009**.
26. "Great interest in pilot plant for nanocellulose production", In Beyond. Norsborg: Innventia AB, **2010**, 8.
27. "Forest Products Laboratory sets up pilot plant for wood-derived nanocellulose", Add. Polym., **2012**, *10*, 7.
28. Wiliamson, M. "Nanocellulose - on the cusp of commercialization?" International Paper World, **2012**, *10*, 11, 31–36.
29. Melody, B. In C&E News; **2014**, *92*, 7, American Chemical Society.
30. Jacoby, M. Nano from the forest. C&E News June 30, **2014**, American Chemical Society.
31. Jorfi, M.; Roberts, M. N.; Foster, E. J.; Weder, C. *ACS Appl. Mater. Interfaces* **2013**, *5*, 1517.
32. Way, A. E.; Hsu, L.; Shanmuganathan, K.; Weder, C.; Rowan, S. *J. ACS Macro Lett.* **2012**, *1*, 1001.
33. Capadona, J. R.; Shanmuganathan, K.; Tyler, D. J.; Rowan, S. J.; Weder, C. *Science* **2008**, *319*, 1370.
34. Shanmuganathan, K.; Capadona, J. R.; Rowan, S. J.; Weder, C. *J. Mater. Chem.* **2010**, *20*, 180.
35. Rusli, R.; Shanmuganathan, K.; Rowan, S. J.; Weder, C.; Eichhorn, S. *J. Biomacromolecules* **2010**, *11*, 762.
36. Mendez, J.; Annamalai, P. K.; Eichhorn, S. J.; Rusli, R.; Rowan, S. J.; Foster, E. J.; Weder, C. *Macromolecules* **2011**, *44*, 6827.
37. Wang, H.; Roman, M. *Biomacromolecules* **2011**, *12*, 1585.
38. Lee, J. E.; Lee, N.; Kim, H.; Kim, J.; Choi, S. H.; Kim, J. H.; Kim, T.; Song, I. C.; Park, S. P.; Moon, W. K.; Hyeon, T. *J. Am. Chem. Soc.* **2009**, *132*, 552.

39. Huang, J.; Matsunaga, N.; Shimanoe, K.; Yamazoe, N.; Kunitake, T. *Chem. Mater.* **2005**, *17*, 3513.
40. Habibi, Y.; Hoeger, I.; Kelley, S. S.; Rojas, O. *J. Langmuir* **2009**, *26*, 990.
41. Csoka, L.; Hoeger, I. C.; Rojas, O. J.; Peszlen, I.; Pawlak, J. J.; Peralta, P. N. *ACS Macro Lett.* **2012**, *1*, 867.
42. Zoppe, J. O.; Peresin, M. S.; Habibi, Y.; Venditti, R. A.; Rojas, O. *J. ACS Appl. Mater. Interfaces* **2009**, *1*, 1996.
43. Dugan, J. M.; Gough, J. E.; Eichhorn, S. *J. Biomacromolecules* **2010**, *11*, 2498.
44. Biyani, M. V.; Foster, E. J.; Weder, C. *ACS Macro Lett.* **2013**, *2*, 236.
45. Coulibaly, S.; Roulin, A.; Balog, S.; Biyani, M. V.; Foster, E. J.; Rowan, S. J.; Fiore, G. L.; Weder, C. *Macromolecules* **2013**, *47*, 152.
46. Lin, N.; Dufresne, A. *Nanoscale* **2014**, *6*, 5384.
47. Tingaut, P.; Zimmermann, T.; Sebe, G. *J. Mater. Chem.* **2012**, *22*, 20105.
48. Paralikar, S. A.; Simonsen, J.; Lombardi, J. *J. Membr. Sci.* **2008**, *320*, 248.
49. Belbekhouche, S.; Bras, J.; Siqueira, G.; Chappey, C.; Lebrun, L.; Khelifi, B.; Marais, S.; Dufresne, A. *Carbohydr. Polym.* **2011**, *83*, 1740.
50. Khan, A.; Khan, R. A.; Salmieri, S.; Le Tien, C.; Riedl, B.; Bouchard, J.; Chauve, G.; Tan, V.; Kamal, M. R.; Lacroix, M. *Carbohydr. Polym.* **2012**, *90*, 1601.
51. Ma, H.; Burger, C.; Hsiao, B. S.; Chu, B. *Biomacromolecules* **2011**, *12*, 970.
52. Fortunati, E.; Armentano, I.; Zhou, Q.; Iannoni, A.; Saino, E.; Visai, L.; Berglund, L. A.; Kenny, J. M. *Carbohydr. Polym.* **2012**, *87*, 1596.
53. Dong, S.; Roman, M. *J. Am. Chem. Soc.* **2007**, *129*, 13810.
54. Zhou, C.; Wu, Q.; Yue, Y.; Zhang, Q. *J. Colloid Interfaces Sci.* **2011**, *353*, 116.
55. Duran, N.; Paula Lemes, A.; Seabra, A. B. *Recent Patents Nanotechnol.* **2012**, *6*, 16.
56. La Mantia, F. P.; Morreale, M. *Compos. Part A: Appl. Sci. Manuf.* **2011**, *42*, 579.
57. Mariano, M.; El Kissi, N.; Dufresne, A. *J. Polym. Sci. Part B: Polym. Phys.* **2014**, *52*, 791.
58. Capadona, J. R.; Van Den Berg, O.; Capadona, L. A.; Schroeter, M.; Rowan, S. J.; Tyler, D. J.; Weder, C. *Nat. Nanotechnol.* **2007**, *2*, 765.
59. Hussain, F.; Hojjati, M.; Okamoto, M.; Gorga, R. E. *J. Compos. Mater.* **2006**, *40*, 1511.
60. Kumar, S.; Hofmann, M.; Steinmann, B.; Foster, E. J.; Weder, C. *ACS Appl. Mater. Interfaces* **2012**, *4*, 5399.
61. Goffin, A. L.; Raquez, J. M.; Duquesne, E.; Siqueira, G.; Habibi, Y.; Dufresne, A.; Dubois, P. *Polymer* **2011**, *52*, 1532.
62. Bondeson, D.; Oksman, K. *Compos. Part A: Appl. Sci. Manufact.* **2007**, *38*, 2486.
63. Alloin, F.; D'Aprea, A.; Dufresne, A.; Kissi, N.; Bossard, F. *Cellulose* **2011**, *18*, 957.
64. Sapkota, J.; Kumar, S.; Weder, C.; Foster, E. *J. Macromol. Mater. Eng.* **2015**, *300*, 562.
65. Wang, N.; Ding, E.; Cheng, R. *Polymer* **2007**, *48*, 3486.
66. Sapkota, J.; Jorfi, M.; Weder, C.; Foster, E. *J. Macromol. Rapid Commun.* **2014**, *35*, 1747.
67. Camarero Espinosa, S.; Kuhnt, T.; Foster, E. J.; Weder, C. *Biomacromolecules* **2013**, *14*, 1223.
68. Roman, M.; Winter, W. T. *Biomacromolecules* **2004**, *5*, 1671.
69. Markarian, J. *Plast. Addit. Compound.* **2005**, *7*, 18.
70. Kai, H.; Sasho, S.; Munekuni, H. U.S. Patent 12/598,267, 25 June **2013**.
71. Salazar, A.; Rico, A.; Rodríguez, J.; Segurado Escudero, J.; Seltzer, R.; Martin de la Escalera Cutillas, F. *Eur. Polym. J.* **2014**, *59*, 36.
72. Alexandre, B.; Langevin, D.; Médéric, P.; Aubry, T.; Couderc, H.; Nguyen, Q. T.; Saiter, A.; Marais, S. *J. Membr. Sci.* **2009**, *328*, 186.
73. Tong, M.; Yuan, S.; Long, H.; Zheng, M.; Wang, L.; Chen, J. *J. Contam. Hydrol.* **2011**, *122*, 16.
74. Peralta, C. M.; Fernández, L. P.; Masi, A. N. *Microchem. J.* **2011**, *98*, 39.
75. Kurokawa, M.; Uchiyama, Y.; Iwai, T.; Nagai, S. *Wear* **2003**, *254*, 468.
76. Saengthaveep, S.; Magaraphan, R. *Adv. Polym. Technol.* **2013**, *32*, 21352.
77. McKeen, L. W. In Effect of Temperature and Other Factors on Plastics and Elastomers 3rd ed.; McKeen, L. W., Ed.; William Andrew Publishing: Oxford, **2014**; p 233.
78. Drobny, J. G. In Handbook of Thermoplastic Elastomers, 2nd ed.; Drobny, J. G., Ed.; William Andrew Publishing: Oxford, **2014**; p 255.
79. Gupta, B.; Grover, N.; Viju, S.; Saxena, S. In Polyesters and Polyamides; Deopura, B. L., Alagirusamy, R., Joshi, M., Gupta, B., Eds.; Woodhead Publishing: Cambridge, **2008**.
80. Stoeffler, K.; Utracki, L. A.; Simard, Y.; Labonté, S. *J. Appl. Polym. Sci.* **2013**, *130*, 1959.
81. Stoclet, G.; Sclavons, M.; Devaux, J. *J. Appl. Polym. Sci.* **2013**, *127*, 4809.
82. Chen, J. H.; Schulz, E.; Bohse, J.; Hinrichsen, G. *Compos. Part A: Appl. Sci. Manuf.* **1999**, *30*, 747.
83. Coleman, J. N.; Khan, U.; Blau, W. J.; Gun'ko, Y. K. *Carbon* **2006**, *44*, 1624.
84. Roh, S. C.; Kim, J.; Kim, C. K. *Carbon* **2013**, *60*, 317.
85. Pan, Y.-X.; Yu, Z.-Z.; Ou, Y.-C.; Hu, G.-H. *J. Polym. Sci. Part B: Polym. Phys.* **2000**, *38*, 1626.
86. Xu, Z.; Gao, C. *Macromolecules* **2010**, *43*, 6716.
87. Kiziltas, A.; Nazari, B.; Gardner, D. J.; Bousfield, D. W. *Polymer Eng. Sci.* **2013**, 739.
88. Panaitescu, D. M.; Frone, A. N.; Nicolae, C. *Eur. Polym. J.* **2013**, *49*, 3857.
89. Corrêa, A.; de Morais Teixeira, E.; Carmona, V.; Teodoro, K.; Ribeiro, C.; Mattoso, L.; Marconcini, J. *Cellulose* **2014**, *21*, 311.

90. Mueller, S.; Weder, C.; Foster, E. *J. RSC Adv.* **2014**, *4*, 907.
91. Annamalai, P. K.; Dagnon, K. L.; Monemian, S.; Foster, E. J.; Rowan, S. J.; Weder, C. *ACS Appl. Mater. Interf.* **2013**, *6*, 967.
92. Capadona, J. R.; Shanmuganathan, K.; Trittschuh, S.; Seidel, S.; Rowan, S. J.; Weder, C. *Biomacromolecules* **2009**, *10*, 712.
93. Favier, V.; Chanzy, H.; Cavaille, J. Y. *Macromolecules* **1995**, *28*, 6365.
94. Schyrr, B.; Pasche, S.; Voirin, G.; Weder, C.; Simon, Y. C.; Foster, E. *J. ACS Appl. Mater. Interf.* **2014**, *6*, 12674.
95. Ureña-Benavides, E. E.; Ao, G.; Davis, V. A.; Kitchens, C. L. *Macromolecules* **2011**, *44*, 8990.
96. Dagnon, K. L.; Shanmuganathan, K.; Weder, C.; Rowan, S. *J. Macromolecules* **2012**, *45*, 4707.
97. Tang, L.; Weder, C. *ACS Appl. Mater. Interf.* **2010**, *2*, 1073.
98. Li, S.; Li, C.; Li, C.; Yan, M.; Wu, Y.; Cao, J.; He, S. *Polym. Degrad. Stab.* **2013**, *98*, 1940.
99. Jia, X.; Chen, Y.; Shi, C.; Ye, Y.; Wang, P.; Zeng, X.; Wu, T. *J. Agric. Food Chem.* **2013**, *61*, 12405.
100. Lin, N.; Huang, J.; Chang, P. R.; Feng, J.; Yu, J. *Carbohydr. Polym.* **2011**, *83*, 1834.
101. Mendez, J.; Annamalai, P. K.; Eichhorn, S. J.; Rusli, R.; Rowan, S. J.; Foster, E. J.; Weder, C. *Macromolecules* **2011**, *44*, 6827.
102. Biyani, M. V.; Weder, C.; Foster, E. J. *Polym. Chem.* **2014**, *5*, 5501.
103. Takayanagi, M.; Uemura, S.; Minami, S. *J. Polym. Sci. C* **1964**, *5*, 113.
104. Ouali, N.; Cavaille, J. Y.; Perez, J. *Plast. Rubber Comp. Process. Appl.* **1991**, *16*, 55.
105. Kiziltas, A.; Gardner, D. J.; Han, Y.; Yang, H.-S. *Thermochim. Acta* **2011**, *519*, 38.
106. Tang, L. M.; Weder, C. *ACS Appl. Mater. Interfaces* **2010**, *2*, 1073.
107. Capadona, J. R.; van den Berg, O.; Capadona, L.; Schroeter, M.; Tyler, D.; Rowan, S. J.; Weder, C. *Nat. Nanotechnol.* **2007**, *2*, 765.
108. Bras, J.; Viet, D.; Bruzzese, C.; Dufresne, A. *Carbohydr. Polym.* **2011**, *84*, 211.